

Phase transition extracted by principal component analysis in the disordered Moore-Read state

Na Jiang(江娜), Shuaixin Fu(付帅鑫), Zhengzhi Ma(马正直), and Lian Wang(王莲)

Citation: Chin. Phys. B, 2025, 34 (**4**): 047306. DOI: 10.1088/1674-1056/adb25f
Journal homepage: http://cpb.iphy.ac.cn; http://iopscience.iop.org/cpb

What follows is a list of articles you may be interested in

Phase transition in bilayer quantum Hall system with opposite magnetic field

Ke Yang(杨珂)
Chin. Phys. B, 2023, 32 (**9**): 097303. DOI: 10.1088/1674-1056/ace61d

Entanglement spectrum of non-Abelian anyons

Ying-Hai Wu(吴英海)
Chin. Phys. B, 2022, 31 (**3**): 037302. DOI: 10.1088/1674-1056/ac280d

Neutral excitation and bulk gap of fractional quantum Hall liquids in disk geometry

Wu-Qing Yang(杨武庆), Qi Li(李骐), Lin-Peng Yang(杨林鹏), Zi-Xiang Hu(胡自翔)
Chin. Phys. B, 2019, 28 (**6**): 067303. DOI: 10.1088/1674-1056/28/6/067303

Behavior of fractional quantum Hall states in LLL and 1LL with in-plane magnetic field and Landau level mixing: A numerical investigation

Lin-Peng Yang(杨林鹏), Qi Li(李骐), Zi-Xiang Hu(胡自翔)
Chin. Phys. B, 2018, 27 (**8**): 087306. DOI: 10.1088/1674-1056/27/8/087306

Exotic electronic states in the world of flat bands： From theory to material

Liu Zheng (刘峥), Liu Feng (刘锋), Wu Yong-Shi (吴咏时)
Chin. Phys. B, 2014, 23 (**7**): 077308. DOI: 10.1088/1674-1056/23/7/077308

Phase transition extracted by principal component analysis in the disordered Moore–Read state

Na Jiang(江娜)[1,2,†], Shuaixin Fu(付帅鑫)[1], Zhengzhi Ma(马正直)[1], and Lian Wang(王莲)[1]

[1] *School of Materials Science and Engineering, Chongqing Jiaotong University, Chongqing* 400074, *China*
[2] *Southwest Center for Theoretical Physics, Chongqing University, Chongqing* 401331, *China*

(Received 21 October 2024; revised manuscript received 18 January 2025; accepted manuscript online 5 February 2025)

We study the influence of disorder on the Moore–Read state by principal component analysis (PCA), which is one of the ground state candidates for the 5/2 fractional Hall state. By using PCA, the topological features of the ground state wave functions with different disorder strengths can be distilled. As the disorder strength increases, the Moore–Read state will be destroyed. We explore the phase transition by analyzing the overlaps between the random sample wave functions and the topologically distilled state. The cross-point between the amplitudes of the principal component and its counterpart is the phase transition point. Additionally, the origin of the second component comes from the excited states, which is different from the Laughlin state.

Keywords: fractional quantum Hall, phase transition, principal component analysis

PACS: 73.43.Nq, 64.70.Tg, 05.30.Rt

DOI: 10.1088/1674-1056/adb25f **CSTR:** 32038.14.CPB.adb25f

1. Introduction

The fractional quantum Hall effect remains one of the most interesting strongly correlated systems for electrons moving in an effective two-dimensional manifold.[1] Generally speaking, the ground states of the fractional quantum Hall (FQH) liquid are incompressible and exhibit topological order, a form of order that does not rely on any symmetry of the system.[2] The most powerful numerical tool for studying the FQH states is exact diagonalizing a microscopic Hamiltonian for a small number of electrons or other advanced numerical methods, such as the density-matrix renormalization group (DMRG) invented by White[3–8] or the matrix-product state (MPS).[9] Theoretically, the numerical calculation can be applied to different geometries for different purposes. For a sphere or a torus, we typically investigate the bulk topological properties, unaffected by edge effects, including the ground state topological degeneracy and magneto-roton excitations.[10–12] For disk or cylinder geometries, we can study edge physics,[13] such as edge reconstruction,[14–18] quasi-particle interference[19–29] and edge tunneling.[30–36] However, for disk geometry, it can also be utilized to investigate bulk properties in recent research, such as the bulk gap and collective magneto-roton excitations.[37,38] The bulk energy gap can be obtained between the lowest two states within the center of mass system.

Different FQH states can be represented by model wave functions, which are typically derived by diagonalizing the pseudopotential Hamiltonians introduced by Haldane[39] and Jack polynomials, which are homogeneous symmetric polynomials specified by a rational parameter and a root configuration.[40] For example, for the unambiguous Laughlin state, which can be obtained from the model Hamiltonian with V_1 interaction, its spectrum of magneto-roton excitations exactly match those from the sphere geometry. For a non-Abelian FQH state, such as a Moore–Read state at $\nu = 5/2$, it can be derived by diagonalizing the model Hamiltonian with V_3 interaction, whose nature has been debated since its discovery three decades ago,[41] a Majorana neutral mode exists which is the heart of its non-Abelian topology. It is different from a Laughlin state, whose topological properties are reflected through the edge mode counting[42] and the structure of the entanglement spectrum.[43] However, the electrons interact via the Coulomb potential supplemented with modifications such as finite sample width and Landau level mixing in experiments. Furthermore, disorders are essential for the quantum Hall plateau and they give rise to a corresponding effective potential. Due to these reasons, there are some ground state candidates for $\nu = 5/2$, such as the Moore–Read Pfaffian state, the anti-Pfaffian state and the particle–hole Pfaffian state. The interaction is always anisotropic in realistic systems. The interaction anisotropy can also be an in-plane magnetic field, thereby disrupting the symmetry of the system and introducing an additional degree of freedom.[44] For a Laughlin state, the model wave function corresponding to the anisotropy can be obtained by unimodular transformation of the isotropic ground state.[45] The anisotropy factor can also be obtained by principal component analysis (PCA).[46] When the anisotropy is

†Corresponding author. E-mail: 990202000072@cqjtu.edu.cn

© 2025 Chinese Physical Society and IOP Publishing Ltd. All rights, including for text and data mining, AI training, and similar technologies, are reserved.

large enough, the system transitions to another phase and the spectral gap is closed. For a disorder effect, the strength is weak and the topological properties of the ground state are robust. When the disorder strength is comparable to the electrons' interaction, the ground states will be destroyed and the phase transition occurs. Meanwhile, when the mobility gap closes, the topological Chern number calculation[47] shows that the phase transition occurred. Also, a collapse of degeneracy and a crossing of energy levels can characterize the phase transition point.[48] For a Laughlin state, many methods can detect this phase transition, such as disordered-averaged entanglement entropy and level statistics.[49–52] Can we explore the phase transition for a non-Abelian 5/2 state, such as the Moore–Read state? In fact, all the information is involved in the ground state. For example, we can calculate fidelity[51] and tunneling matrix element[53] of a Laughlin state from its ground state. So, we can explore the phase transition of a Moore–Read state with a disorder effect in its ground state momentum subspace.

At the same time, the development of machine learning (ML)[54] has brought new research methods to various fields. It can be used to identify phases and phase transitions.[55,56] For large amounts of data from complex systems, ML can effectively identify the relationships between them. Moreover, unsupervised ML can reveal hidden features without labelling.[57] PCA, which is a type of unsupervised ML, has been shown to effectively discriminate different phases.[58] Now, it has been used to identify the phase transition of a $\nu = 1/3$ quantum Hall state.[59] In this paper, we will explore the phase transition of a Moore–Read state with rotational disorder on the disk geometry by using PCA. We can study the bulk phase transition on the disk because the spectrum of the magneto-roton excitation exactly matches that of the sphere geometry. The energy gap can be obtained by the energy difference between the first excited state and the ground state in the ground state angular momentum sector. We feed the ground state wave functions into the PCA, which are obtained by diagonalizing the model Hamiltonian with different disorder strengths. Then we show a way to extract the phase transition point from the Moore–Read FQH state to the insulator. At the same time, the ground state wave functions with disorder have more complex impact factors. We can identify the lower and higher energy excitations in the clean energy spectrum by PCA, with results that are different from the Laughlin state.

The rest of this paper is arranged as follows. The model and methods are introduced in Section 2. In Section 3, the topological state can be distilled by wave function overlaps. In Section 4, the critical point is explored from overlaps by PCA, and the results are consistent with the critical disorder strength obtained by using a closed energy gap. In addition, the origins of some principal components are presented. Conclusions and discussions are arranged in Section 5.

2. Model and method

Our model focuses on the Moore–Read state, which was proposed by Moore and Read[60] for a half-filled lowest Landau level or its particle–hole conjugate[61–63] on the disk geometry. The many-body model wave function can be obtained by exactly diagonalizing a model Hamiltonian for a three-body interaction. The wave function for the Moore–Read state is expressed as

$$\begin{aligned}&\Psi_{\mathrm{MR}}(z_1, z_2, z_3, \ldots, z_N)\\ &= \mathrm{Pf}\Big(\frac{1}{z_i - z_j}\Big)\prod_{i<j}(z_i - z_j)^2 \mathrm{e}^{-\sum_i \frac{|z_i|^2}{4}}.\end{aligned} \tag{1}$$

The specific form of the three-body Hamiltonian is[64]

$$H_{3\mathrm{B}} = -\sum_{i<j<k} S_{ijk}[\nabla_i^2 \nabla_j^4 \delta(\boldsymbol{r}_i - \boldsymbol{r}_j)\delta(\boldsymbol{r}_i - \boldsymbol{r}_k)], \tag{2}$$

where S_{ijk} is a symmetric operator defined as $S_{123}[f_{123}] = f_{123} + f_{231} + f_{321}$. In the actual system, the three-body interaction comes from Landau level mixing. In addition, the three-body Hamiltonian can also be represented by the projection operator

$$H_{3\mathrm{B}} = \sum_M \sum_{i<j<k} |\psi_M(i,j,k)\rangle\langle\psi_M(i,j,k)|, \tag{3}$$

$\psi_M(i,j,k)$ is three-body wave function

$$\psi_M(z_1, z_2, z_3) = B_M(z_1 + z_2 + z_3)^{M-3} J(z_1, z_2, z_3), \tag{4}$$

where $J(z_1, z_2, z_3) = (z_1 - z_2)(z_1 - z_3)(z_2 - z_3)$ is the Jastrow factor and the normalization factor B_M is

$$B_M = \frac{1}{(2\pi)^{3/2}}\sqrt{\frac{3^{M-4}}{2^{M+2}(M-3)!}}, \tag{5}$$

the M is total angular momentum. After the second quantization, the three-body Hamiltonian can be expressed in the occupation number space as

$$\begin{aligned}H_{3\mathrm{B}} = &\sum_{m_1<m_2<m_3}\sum_{m_4<m_5<m_6} U(\{m_i\})\\ &\times c_{m_1}^\dagger c_{m_2}^\dagger c_{m_3}^\dagger c_{m_4} c_{m_5} c_{m_6},\end{aligned} \tag{6}$$

where $U(\{m_i\})$ is the coefficient. The total angular momentum $M = m_1 + m_2 + m_3$. For an N-electron system, the total angular momentum of the Moore–Read state is $M_{\mathrm{MR}} = N(2N-3)/2$.

In general, the translational symmetry of the system is broken after introducing the disorder. We always need to do sample averaging and the translational symmetry recovers when the disorder is randomly distributed and the number of

the disorder is large enough. Here, for simplicity, we consider an uncorrelated random potential

$$H_{\mathrm{D}} = \sum_m U_m c_m^{\dagger} c_m, \tag{7}$$

where U_m is a random number by uniform distribution in the range $[-W, W]$. This potential maintains rotational symmetry because we assume that the disorder effects are averaged firstly in each Landau orbit. It ensures that the total angular momentum remains a good quantum number. We will focus on the ground state angular momentum sector of the Moore–Read state to explore its disorder effect.

PCA can reduce the dimension of data and extract the principal information. In this work, we feed the ground state wave functions with different disorders to PCA as input data. The disordered wave functions can be expressed as

$$|\Psi_{\mathrm{sample}}\rangle = |\psi^{W_m^n}\rangle = \sum_{i=1}^{D} c_i^{W_m^n} |i\rangle. \tag{8}$$

Here, m is the index number of disorder strength and n is the sample index, and D is the dimension of Hilbert space. We can construct a matrix of $(M \times N) \times D$, where M is the number of disorder strengths, and N is the number of samples for each disorder strength. The input matrix can be obtained as

$$\boldsymbol{X} = \begin{pmatrix} c_1^{W_1^1} & c_2^{W_1^1} & \cdots & c_D^{W_1^1} \\ \vdots & \vdots & \cdots & \vdots \\ c_1^{W_1^N} & c_2^{W_1^N} & \cdots & c_D^{W_1^N} \\ c_1^{W_2^1} & c_1^{W_2^1} & \cdots & c_D^{W_2^1} \\ \vdots & \vdots & \cdots & \vdots \\ c_1^{W_2^N} & c_1^{W_2^N} & \cdots & c_D^{W_2^N} \\ \vdots & \vdots & \cdots & \vdots \\ c_1^{W_M^N} & c_2^{W_M^N} & \cdots & c_D^{W_M^N} \end{pmatrix}. \tag{9}$$

PCA is similar to singular value decomposition (SVD). Using SVD to decompose the $\boldsymbol{X}$ matrix,

$$\boldsymbol{X} = \boldsymbol{U}\boldsymbol{\Sigma}\boldsymbol{V}^{\mathrm{T}}, \tag{10}$$

where $\boldsymbol{V}$ is a $D \times D$ matrix which contains the eigenvectors of matrix $\boldsymbol{X}\boldsymbol{X}^{\mathrm{T}}$. $\boldsymbol{\Sigma}$ is a diagonal matrix whose diagonal elements squared are the eigenvalues of $\boldsymbol{X}\boldsymbol{X}^{\mathrm{T}}$. The eigenvalues are called the explained variance ratios (EVRs).

To study the disorder effect of the Moore–Read state, we will focus on two situations. The first one is that we feed ground state wave functions with a fixed disorder strength to PCA and the second situation is that we feed the ground state wave functions with mixed disorder strengths

$$\boldsymbol{X} = \begin{pmatrix} W_{0.1} \\ W_{0.2} \\ \vdots \\ W_{\mathrm{s}} \end{pmatrix}$$

to PCA. The former can extract topological information with different disorder strengths. Meanwhile, the latter can identify the critical phase transition point of the Moore–Read state with a disorder effect.

3. Topological state distillation

To explore the disorder effect of the Moore–Read state, we plot the histograms of the overlaps between disordered ground state wave functions and the Moore–Read state wave function. For a 10-electron system, we have studied more than 1000 sample overlaps. As shown in Fig. 1(a), the frequencies are predominantly distributed within the range [0.99, 1.0] for $W = 0.20$ strength, with a peak at 0.997 and a slight leftward tail. This indicates that the Moore–Read state is robust with small disorder strength. In contrast, Fig. 1(b) shows the histogram for $W = 2.90$, where the frequencies are concentrated in the range [0.0, 0.2], with a peak at 0.0 and a long rightward tail. This distribution demonstrates that the Moore–Read state is destroyed with a larger disorder strength and transitions to a new phase. The significant difference between these two histograms indicates a phase transition occurring between disorder strength $W = 0.20$ and $W = 2.90$.

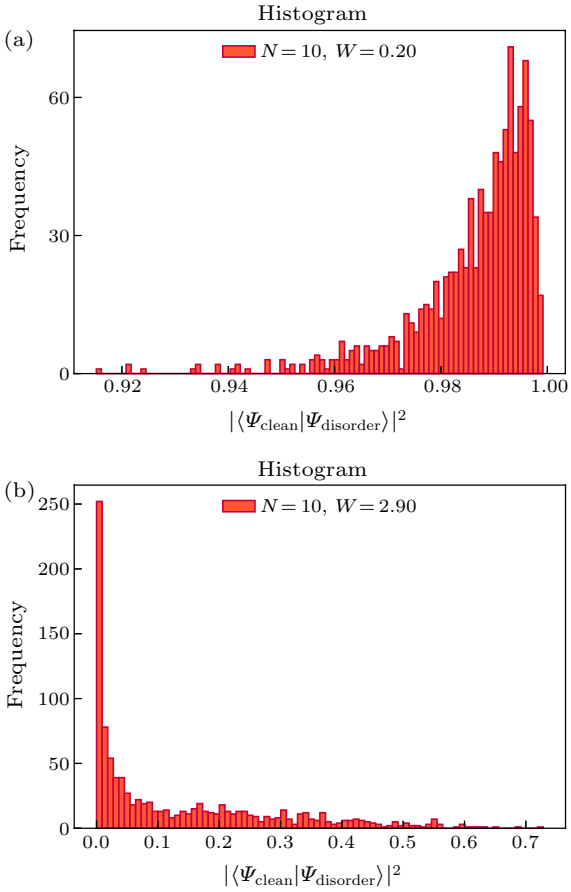


Fig. 1. For a 10-electron system, the histograms of the overlaps between the Moore–Read state and the ground states with disorder strengths $W = 0.20$ (a) and 2.90 (b). More than 1000 samples are studied.

Take a 10-electron system as an example, as shown in Fig. 2. The first ten (EVRs) λ_i are plotted. Figure 2(a) is plotted with disorder strength $W = 0.20$, the first EVRs $\lambda_1 = 0.77$ are much larger than the second EVRs $\lambda_2 = 0.071$ and the others are nearly zero. The inset plot shows the first five logarithmic EVRs for straightforward comparison. Figure 2(b) is plotted with disorder strength $W = 2.90$, the first EVRs λ_1 are still larger than the other values; however, all values are smaller than the results in Fig. 2(a). The wave function Ψ_{λ_i} is the ith component, which is the ith column of $\boldsymbol{V}^{\mathrm{T}}$ for SVD. For the most important component, which is the first component in two cases, is it a topological state analogous to a Laughlin state? So, we study the overlaps between the first component wave function and the Moore–Read state wave function. The two results are close to 1 for disorder strength $W = 0.20$ and $W = 2.90$. It gives us a hint that we can extract the topological Moore–Read state from disordered states, even if the disorder states have negligible overlaps with the Moore–Read state.

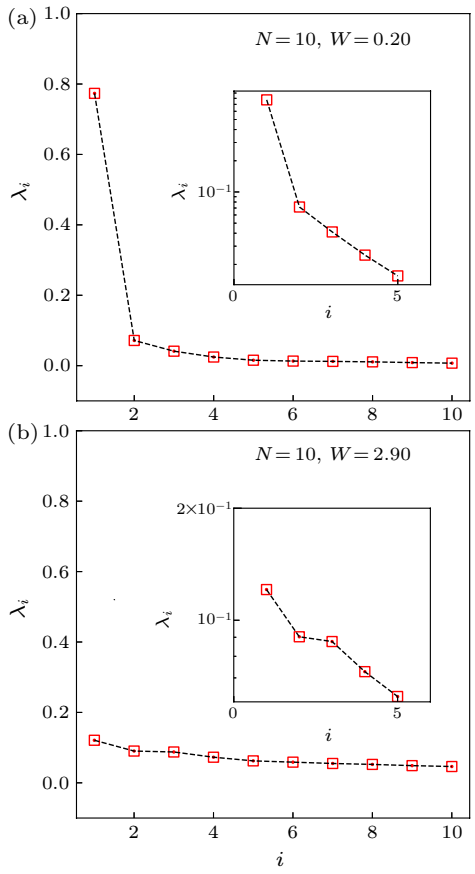


Fig. 2. For a 10-electron system, the EVRs are plotted for fixed disorder strengths. The first ten EVRs are plotted for $W = 0.20$ in (a) and $W = 2.90$ in (b). The inset plot shows the first five logarithmic EVRs, respectively.

To verify that the topological Moore–Read state can be extracted, we have studied the overlaps between the Moore–Read state and the first component obtained from different disordered systems, such as an $(N = 6, 8, 10, 12)$ electrons system with different disorder strengths $(W = 0.20, 0.50, 0.80, \ldots, 2.60)$. These results are shown in Fig. 3. For the different system sizes with smaller disorder strength, the overlap values $|\langle\Psi_{\mathrm{MR}}|\Psi_{\lambda_1}\rangle|^2$ are 0.99 or even close to 1. Interestingly, the overlap values are still larger than 0.95 for stronger disorders, which have almost 0 overlaps between the Moore–Read state and disordered states. In these finite systems, we could conclude that the Moore–Read state can be distilled in disordered states by PCA. The PCA can facilitate the uncovering of latent topological information in a non-Abelian quantum Hall state.

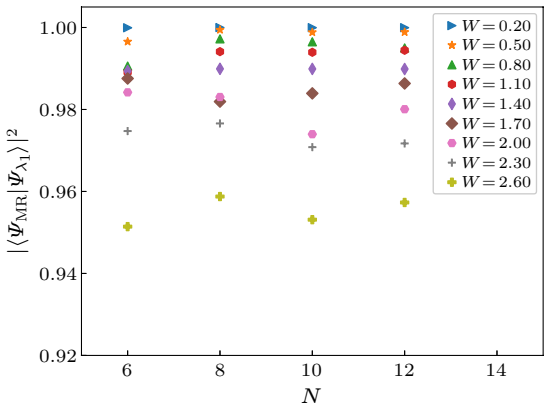


Fig. 3. The overlaps between the Moore–Read state Ψ_{MR} and the first component Ψ_{λ_1} are analyzed for different disorder strengths $(W = 0.20, 0.50, 0.80, \ldots, 2.60)$ and different system sizes $(N = 6, 8, 10, 12)$. The y-axis presents the overlap values $|\langle\Psi_{\mathrm{MR}}|\Psi_{\lambda_1}\rangle|^2$, ranging from 0.92 to 1. Different disorder strengths are plotted with different colors.

4. Quantum phase transition of the Moore–Read state

In the previous section, we have discussed that PCA can extract the topological state (Moore–Read state) in disordered states. However, the histogram in Fig. 1 shows that the ground state has changed with a larger disorder strength. Meanwhile, the critical disorder strength falls within the range of [0.20, 2.90] and the ground states have a corresponding phase transition. For exploring ground state phase transitions, we feed the mixed disordered ground states into PCA. The disorder strengths vary from 0.1 to 2.9 with an interval of 0.1. For each disorder strength, there are more than 1000 samples, which are calculated by diagonalizing the model Hamiltonian in ground state space. As shown in Fig. 4(a), the first EVRs for each disorder strength are plotted. The values decrease smoothly as the disorder strengths increase. It shows that the ground state will be destroyed from a topological state to another state. It seems that all the components cannot be negligible with a strong enough disorder strength. We can find the results in Fig. 4(b), where EVRs for mixed disorder strength until $W_{\mathrm{s}} = 2.90$ are plotted. At the same time, we know that the first leading component Ψ_{λ_1} contains the dominating features in the mixed disordered dataset and the dominating feature is the topological Moore–Read state.

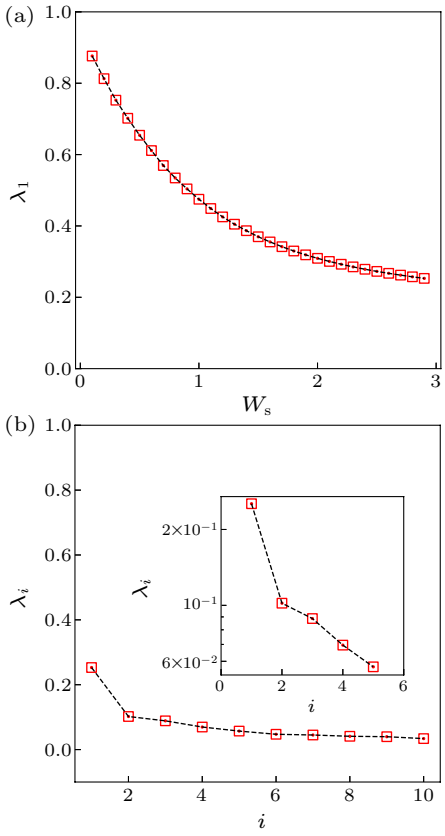


Fig. 4. For a 10-electron system, more than 1000 samples for each disorder strength have been fed to the PCA to extract the components. The input dataset is mixed disorder strengths. (a) The first EVRs λ_1 as a function of mixed disorder strength. (b) The EVRs for a mixed disorder strength until $W = 2.90$. The inset plot provides logarithmic-scale EVRs for the first five principal components.

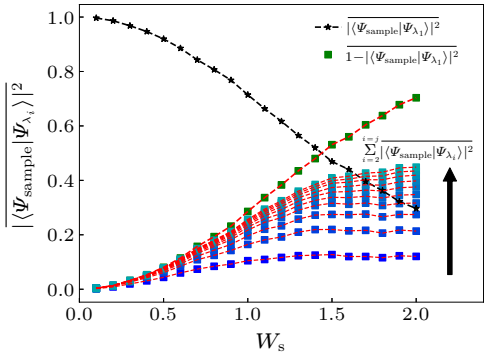


Fig. 5. Averaged sample projection square to the leading components. The black stars represent the averaged amplitudes of the sample wave functions on the first principal component wave function $\overline{|\langle\Psi_{\rm sample}|\Psi_{\lambda_1}\rangle|^2}$. The green squares represent the sum of the averaged amplitudes of the sample wave functions on the other principal component wave functions $1-\overline{|\langle\Psi_{\rm sample}|\Psi_{\lambda_1}\rangle|^2}$. The blue-green gradient squares are the sum of averaged amplitudes from the second principal component to jth principal component $\sum_{i=2}^{i=j}\overline{|\langle\Psi_{\rm sample}|\Psi_{\lambda_i}\rangle|^2}$.

Physically, PCA redistributes the data into a new set of complete basis $|\Psi_{\lambda_i}\rangle$. The quantity $|\langle\Psi_{\rm sample}|\Psi_{\lambda_i}\rangle|^2$ can be named as the amplitudes of the principal components. Due to a large amount of samples, the amplitudes need to be averaged over all samples as $\overline{|\langle\Psi_{\rm sample}|\Psi_{\lambda_i}\rangle|^2}$. We investigate the amplitudes in each disorder sector separately. The value of amplitude drop to 50% means that the ground state has been destroyed by the disorder from the first leading component to some other components. In this section, we turn to the amplitudes of the principal components $\overline{|\langle\Psi_{\rm sample}|\Psi_{\lambda_i}\rangle|^2}$ to study the phase transition. For a 10-electron system, the ground state wave functions of twenty disorder strengths vary within the range from 0.1 to 2.0, with an interval of 0.1. The mixed disorder wave function dataset is fed to the PCA separately and twenty averaged amplitudes can be obtained. In Fig. 5, we plot the curve of the amplitudes. As an example, the black stars are the averaged amplitudes of the first component $\overline{|\langle\Psi_{\rm sample}|\Psi_{\lambda_1}\rangle|^2}$. As disorder strength increases, the averaged amplitudes decrease. It means that the importance of other components increases. Then we plot the sum of averaged amplitudes from the second to ith components in green squares. Because the new basis $|\Psi_{\lambda_i}\rangle$ is complete, the sum of averaged amplitudes is exactly $1-\overline{|\langle\Psi_{\rm sample}|\Psi_{\lambda_1}\rangle|^2}$ as i is the dimension of the ground state space. We can see that the values of the sum averaged amplitudes increase with increasing disorder strength. In addition, the sum of the averaged amplitudes of the first ten components $\overline{|\langle\Psi_{\rm sample}|\Psi_{\lambda_i}\rangle|^2}$ are shown from dark-blue to green squares. The curves of $\overline{|\langle\Psi_{\rm sample}|\Psi_{\lambda_1}\rangle|^2}$ and $1-\overline{|\langle\Psi_{\rm sample}|\Psi_{\lambda_1}\rangle|^2}$ have a crossing point. The disorder strength of the crossing point is $W_{\rm s}({\rm PCA}) = 1.436$. It indicates that the state has an equal probability entering the Ψ_{λ_1} or other components Ψ_{λ_i}.

Utilizing the same analytical method for other electronic systems ($N = 6$, 8, 12), the critical disorder strengths $W_{\rm s}({\rm PCA})$ have been obtained. For these finite size system results, we can explore a scaling relation between critical disorder strength $W_{\rm s}({\rm PCA})$ and system size $N = 6$, 8, 10, 12. In the thermodynamic limit as $N \to \infty$, the critical disorder strength can be fitted as shown Fig. 6(a). We try to adopt the polynomial to fit the critical disorder strength for simplification

$$C\left(\frac{1}{N}\right) = 110\left(\frac{1}{N}\right)^2 - 27.11\left(\frac{1}{N}\right) + 3.0. \tag{11}$$

The y-intercept $W_{\rm s}({\rm PCA}) = 3.045 \pm 0.046$ is the critical disorder in the thermodynamic limit. This critical value indicates the collapse of the Moore–Read state. These Moore–Read states are obtained by diagonalizing the V_3 interaction. However, the critical disorder strengths of Laughlin $W_{\rm s}({\rm PCA}) \approx 0.4$ are obtained by diagonalizing the V_1 interaction. If we explore the Coulomb interaction in the two cases, we can get the result that it is more difficult to maintain the Moore–Read state.

For comparison, we explore the critical disorder strength with some other methods, such as the energy gap between the first excited state and the ground state. It can be defined as $\Delta E = E_1 - E_0$. We have examined energy gaps with different disorder strengths and different system sizes. For the fixed

disorder strength, more than 1000 ΔE can be averaged in a specific system. For different systems ($N = 6$, 8, 10, 12), we can plot the averaged energy gap $\overline{\Delta E_W}$ with system sizes $(1/N)$. The energy gap of the thermodynamic limit can be extracted as $\Delta E_W^{\lim}$. As shown in Fig. 6(b), thermodynamic limit energy gaps $\Delta E_W^{\lim}$ of different disorder strengths from 0 to 2.9 have been obtained. After scaling between $\Delta E_W^{\lim}$ and the disorder strength, we can extract the critical disorder in the thermodynamic limit, where the energy gap is closed.

$$\Delta E_W^{\lim} = -0.041 W^{1.38} + 0.2. \tag{12}$$

From Eq. (12), we can get the energy gap closing by solving the x-intercept. The disorder strength can be obtained as $W = 3.132 \pm 0.030$ when the energy gap is closed. The results agree with the PCA result $W_s(\mathrm{PCA}) = 3.045 \pm 0.046$. The results of critical disorder strength in the thermodynamic limit prove that PCA can be used to explore the phase transition for a Moore–Read state.

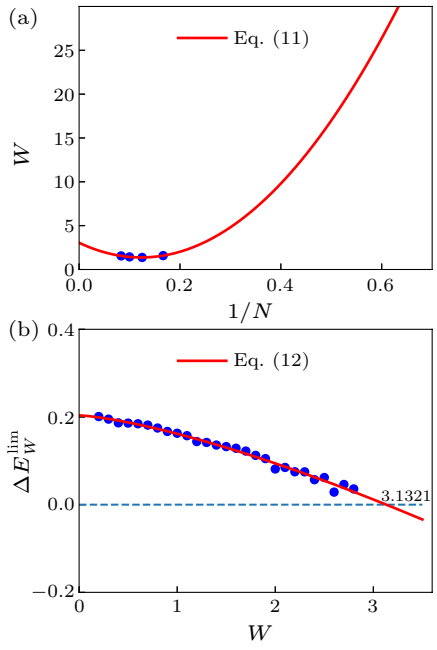


Fig. 6. The critical disorder strengths $W_s(\mathrm{PCA})$ by PCA and energy gaps between the first excited state and the ground state are extracted, respectively. (a) The scaling of $W_s(\mathrm{PCA})$ as a function of $1/N$ with $N = 6$, 8, 10, 12. The critical disorder is $W_s(\mathrm{PCA}) \approx 3.045$ in the thermodynamic limit. (b) The energy gaps in the thermodynamic limit $\Delta E_W^{\lim}$. They are obtained from the scaling of different system sizes for each disorder. Then the critical disorder strength is $W = 3.13$, which means zero energy gap in the thermodynamic limit.

After analyzing the phase transition from overlaps between components and wave functions of samples, we are curious about the origin of these components. In previous sections, we have learned that the first component state Ψ_{λ_1} is the topological Moore–Read state. It can be proven by calculating overlap between Ψ_{λ_1} and the ground state Ψ_{E_1}, for which Ψ_{E_i} are states of the free disorder system in the same momentum sector $M = N(2N-3)/2$. However, what is the origin of the components apart from the topological one? We should notice that we have performed extract diagonalization in individual momentum sectors of the Moore–Read state. So, these components should all come from the same momentum sector. In Fig. 7 we have calculated the overlaps between the first ten components and the states of the free disorder spectrum. The values of the overlaps are labeled using colors. At the same time, the states of the free disorder energy spectrum are labeled using a black bar for comparison. The first components are labeled 1 in x-axis by a red bar. Where are the other components (components $= 2, \ldots, 10$) that contain the remaining information about the dataset? We can find that they come from the low energy excited states, apart from the second component Ψ_{λ_2} in (a). The second component comes from the higher excited state in (b).

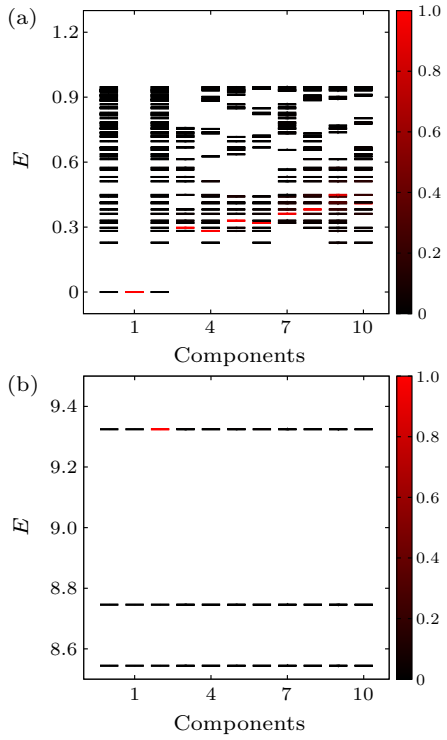


Fig. 7. The origin of the principal components extracted from PCA results in a 10-electron system. The colored bars are the states that have nonzero overlaps $|\langle\Psi_{\lambda_i}|\Psi_{E_i}\rangle|^2$. The states Ψ_{E_i} are the energy spectrum of the free disorder system, which are labeled with a black bar. The colored bars range from 0 to 1. (a) The first ten principal components Ψ_{λ_i} except the second Ψ_{λ_2} are extracted from the lower excitation states. (b) The second principal component Ψ_{λ_2} is extracted from higher excitation states.

5. Conclusion

In conclusion, we have studied the impact of disorder in a Moore–Read state, which is a candidate ground state for an $\nu = 5/2$ fractional quantum Hall system. In previous studies, the critical disorder of a fractional quantum Hall to insulator transition was obtained from the mobility gap. By using the degrees of freedom in the center of mass system, the bulk energy gap can be obtained in disk geometry for the thermodynamic limit. In this study, we have explored the related physics

in a disordered system in disk geometry, such as phase transition and topological state extraction. The main point in this work is the use of an unsupervised machine learning method, i.e., PCA. We can extract physics without labeling input data.

PCA is a useful method to reduce the dimensions of input data. It can be used to extract the dominant characteristic. Firstly, we have studied how topological state can be extracted in disordered systems, regardless of whether the disorder strength is weak or strong. By calculating the overlaps between the first component and the Moore–Read state, it is proven that the first component is the topological Moore–Read state. As we project the input data onto the principal component wave functions, the phase transition can be obtained from the crossing of projections. After doing the same analysis in some even-finite systems, such as $N = 6$, 8, 10, 12 electron systems, the critical disorder approximates as $W_s(\mathrm{PCA}) = 3.045$ in thermodynamic limit, which is consistent with the results obtained from the ground state energy gap results $W = 3.132$. Interestingly, we have found that the other components come from lower excited states, except the second component. This is different from the Laughlin state, where all components come from lower excited states. After analysis of the overlaps between components and the states of a free disorder system, the second component is found to come from a higher excited state. The critical disorder of the Laughlin state approximates to around $W = 0.4$ by analyzing the model Hamiltonian with V_1 interaction. If we study the model of Coulomb interaction with more realistic impurities, the Moore–Read state is typically more difficult to maintain. We will do more related work in the future. We also need to do more work to explore the relationship between components and non-Abelian properties in the future.

Acknowledgements

We thank Zi-xiang Hu for useful discussions. This work was supported by the National Natural Science Foundation of China (Grant Nos. 12104075 and 12347101).

References

[1] Tsui D C, Stormer H L and Gossard A C 1982 *Phys. Rev. Lett.* **48** 1559
[2] Laughlin R B 1983 *Phys. Rev. Lett.* **50** 1395
[3] Shibata N and Yoshioka D 2001 *Phys. Rev. Lett.* **86** 5755
[4] Feiguin A E, Rezayi E, Nayak C and Das Sarma S 2008 *Phys. Rev. Lett.* **100** 166803
[5] Zhao J Z, Sheng D N and Haldane F D M 2011 *Phys. Rev. B* **83** 195135
[6] Hu Z X, Papic Z, Johri S, Bhatt R N and Schmitteckert P 2012 *Phys. Lett. A* **376** 2157
[7] Zeng T S, Hu L D and Zhu W 2022 *Chin. Phys. Lett.* **39** 017301
[8] White S R 1992 *Phys. Rev. Lett.* **69** 2863
[9] Zaletel M P, Mong R S K and Pollmann F 2013 *Phys. Rev. Lett.* **110** 236801
[10] Girvin S M, MacDonald A H and Platzman P M 1985 *Phys. Rev. Lett.* **54** 581
[11] Girvin S M, MacDonald A H and Platzman P M 1986 *Phys. Rev. B* **33** 2481
[12] Yang B, Hu Z X, Papic Z and Haldane F D M 2012 *Phys. Rev. Lett.* **108** 256807
[13] Wen X G 1992 *Int. J. Mod. Phys. B* **6** 1711
[14] MacDonald A H 1990 *Phys. Rev. Lett.* **64** 220
[15] Chamon C de C and Wen X G 1994 *Phys. Rev. B* **49** 8227
[16] Wan X, Rezayi E H and Yang K 2003 *Phys. Rev. B* **68** 125307
[17] Wang J H, Meir Y and Gefen Y 2013 *Phys. Rev. Lett.* **111** 246803
[18] Sabo R, Gurman I, Rosenblatt A, *et al.* 2017 *Nat. Phys.* **13** 491
[19] Fendley P, Fisher M P A and Nayak C 2007 *Phys. Rev. B* **75** 045317
[20] Fradkin E, Nayak C, Tsvelik A and Wilczek F 1998 *Nucl. Phys. B* **516** 704
[21] Das Sarma S, Freedman M and Nayak C 2005 *Phys. Rev. Lett.* **94** 166802
[22] Stern A and Halperin B I 2006 *Phys. Rev. Lett.* **96** 016802
[23] Rosenow B, Halperin B I, Simon S H and Stern A 2008 *Phys. Rev. Lett.* **100** 226803
[24] Bishara B and Nayak C 2008 *Phys. Rev. B* **77** 165302
[25] Bonderson P, Shtengel K and Slingerland J K 2006 *Phys. Rev. Lett.* **97** 016401
[26] Willett R L, Pfeiffer L N and West K W 2009 *Proc. Natl. Acad. Sci. USA* **106** 8853
[27] Willett R L, Pfeiffer L N and West K W 2010 *Phys. Rev. B* **82** 205301
[28] Willett R L, Pfeiffer L N and West K W 2013 arXiv:1301.2594 [cond-mat.mes-hall]
[29] Lin X, Du R R and Xie X C 2014 *National Science Review* **1** 564
[30] Kan C L and Fisher M P A 1992 *Phys. Rev. B* **46** 15233
[31] Moon K, Yi H, Kane C L, Girvin S M and Fisher M P A 1993 *Phys. Rev. Lett.* **71** 4381
[32] Kane C L and Fisher M P A 1994 *Phys. Rev. Lett.* **72** 724
[33] Chamon C de C and Wen X G 1993 *Phys. Rev. Lett.* **70** 2605
[34] Lin X, Dillard C, Kastner M A, Pfeiffer L N and West K W 2012 *Phys. Rev. B* **85** 165321
[35] Li Q, Jiang N, Wan X and Hu Z X 2018 *J. Phys.: Condens. Matter* **30** 255601
[36] Hu Z X, Lee K H, Rezayi E H, Wan X and Yang K 2011 *New J. Phys.* **13** 035020
[37] Yang W Q, Li Q, Yang L P and Hu Z X 2019 *Chin. Phys. B* **6** 067303
[38] Yang Y, Pu S Y, Hu Y Y and Hu Z X 2024 arXiv:2412.02320 [cond-mat.str-el]
[39] Haldane F D M 1983 *Phys. Rev. Lett.* **51** 605
[40] Haldane F D M and Bernevig B A 2008 *Phys. Rev. Lett.* **100** 246802
[41] Willet R L, Eiisenstein J P, Stormer H L, Tsui D C, Gossard A C and English J H 1987 *Phys. Rev. Lett.* **59** 1776
[42] Wen X G 1992 *Int. J. Mod. Phys. B* **6** 1711
[43] Haldane F D M and Li H 1992 *Phys. Rev. Lett.* **101** 010504
[44] Haldane F D M 2008 *Phys. Rev. Lett.* **107** 116801
[45] Haldane F D M, Wan X, Yang K, Yi S and Qiu R Z 2012 *Phys. Rev. B* **85** 115308
[46] Jiang N, Ke S Y, Ji H X, Wang H, Hu Z X and Wan X 2020 *Phys. Rev. B* **102** 115140
[47] Wan X, Rezayi E H, Yang K, Bhatt R N, Haldane F D M and Sheng D N 2003 *Phys. Rev. Lett.* **90** 256802
[48] Yang K 2023 *Chin. Phys. B* **32** 097303
[49] Bhatt R N and Liu Z 2016 *Phys. Rev. Lett.* **117** 206801
[50] Bhatt R N and Liu Z 2017 *Phys. Rev. B* **96** 115111
[51] Sheng D N and Zhu W 2019 *Phys. Rev. Lett.* **123** 056804
[52] Jiang N, Li Q, Zhu Z and Hu Z X 2017 *Annals of Physics* **384** 225
[53] Lu M, Jiang N and Wan X 2019 *Chin. Phys. Lett.* **36** 087301
[54] Cirac I, Cranmer K, Daudet L, Schuld M, Tishby N, Vogt-Maranto L, Zdeborová L and Carleo G 2019 *Rev. Mod. Phys.* **91** 045002
[55] Mehta P, Bukov M, Wang C H, Day A G R, Richardson C, Fisher C K and Schwab D J 2019 *Phys. Rep.* **810** 1
[56] Bedolla E, Padierna L G and Castañeda-Priego R 2021 *J. Phys. Condens. Matter* **33** 053001
[57] Wetzel S J 2017 *Phys. Rev. E* **96** 022140
[58] Zhai H and Wang C. 2017 *Phys. Rev. B* **96** 144432
[59] Jiang N and Lu M 2020 *Chin. Phys. Lett.* **37** 117302
[60] Moore G, Read N and Nucl 1991 *Nucl. Phys. B* **360** 362
[61] Lee S S, Ryu S, Nayak C and Fishaer M P A 2007 *Phys. Rev. Lett.* **99** 236807
[62] Levin M, Halparin B I and Rosenow B 2007 *Phys. Rev. Lett.* **99** 236806
[63] Pakrouski K, Peterson M R, Jolicoeur T, Scarola V W, Nayak C and Troyer M 2015 *Phys. Rev. X* **05** 021004
[64] Greiter M, Wen X G and Wilczak F 1991 *Phys. Rev. Lett.* **66** 3205